Multidecadal regional sea level shifts in the Pacific over 1958–2008

Jae-Hong Moon,[1] Y. Tony Song,[1] Peter D. Bromirski,[2] and Arthur J. Miller[2]

[1] Altimeter data have significantly improved our understanding of regional sea level variability and trends, but their relatively short records do not allow either evaluation of the ocean state prior to 1993 or multidecadal low-frequency signals in the ocean. Here we characterize and quantify the multidecadal regional sea level rise (rSLR) and related ocean heat content in the Pacific from a non-Boussinesq ocean circulation model in comparison with data sets from altimeters, two sea level reconstructions, and in situ ocean profiles from 1958 to 2008. We show that the rSLR trends have undergone two shifts, during the mid-1970s and in the early 1990s, with an east-west dipole pattern in the tropical Pacific. In each of these phases, rSLR accelerated on one side of the Pacific, but decelerated on the other side. The multidecadal sea level shifts can be explained by the dynamical (steric) upper-ocean responses to the surface wind forcing associated with the Pacific Decadal Oscillation (PDO), with negligible contributions from internal (depth-integrated) ocean mass changes. Additional model experimentation further confirms that the Pacific wind stress trend over the recent two decades has played an important role in strengthening the rSLR in the western Pacific while suppressing the rSLR in the eastern Pacific. The climate-forced large-scale rSLR variability is likely to impose a long-term and uneven impact on coastal communities.

1. Introduction

[2] Human-induced and natural trends of sea level are obscured by variability having time scales ranging from seasonal to multidecadal. Among these different time scales, most attention has been given to understanding interannual variability related to the El Niño Southern Oscillation (ENSO), which is particularly relevant to the Pacific Ocean region of interest. Although measuring and understanding interannual and decadal sea level changes have been greatly improved by satellite altimetry data, which have been available since the early 1990s [e.g., *Lee and McPhaden*, 2008; *Church et al.*, 2010], multidecadal and longer sea level variations still remain a challenging issue in diagnosing our climate system.

[3] Long-term tide gauge records from the western tropical Pacific (WTP) indicate that sea level exhibits multidecadal variations that are consistent with the fluctuations observed at Fremantle, Western Australia [e.g., *Feng et al.*, 2004, 2010; *Merrifield*, 2011], showing a relationship with the Southern Oscillation Index (SOI) and the Pacific Decadal Oscillation (PDO) climate indices. Recently, *Merrifield et al.* [2012] reexamined tide gauge data in the WTP and determined that multidecadal sea level trends, including a significant positive trend after early 1990s, are related to Pacific climate indices. They demonstrated that the sea level in the WTP is well explained by global mean sea level (GMSL) and a combination of low-frequency tropical trade wind fluctuations captured by the Pacific climate indices, showing a negative correlation between the WTP sea level and the PDO index. Using a multiple regression analysis with ENSO-related indices, *Merrifield et al.* [2012] also suggested that high-frequency ENSO variability does not account for the recent multidecadal sea level trend in the WTP. Meanwhile, the eastern tropical Pacific (ETP) shows much lower rates of regional sea level rise (rSLR) during the altimetry period (see Figure 1). *Bromirski et al.* [2011] reported virtually no increase of sea levels along the U.S. west coast during the altimetry period, correlating positively with the PDO index. They also focused on the importance of PDO-related wind stress curl in the North Pacific, which can account for the suppression of rSLR along the Pacific coasts of North America. It is known that the Pacific trade winds have experienced a multidecadal weakening trend prior to early 1990s, which was coupled with a shoaling of thermocline associated with the subtropical cells in the WTP [*McPhaden and Zhang*, 2002] and a weakening of the Indonesian through-flow (ITF) [*Wainwright et al.*, 2008; *Feng et al.*, 2011]. On the other hand, the multidecadal rSLR trends reversed since early 1990s, accompanied

[1]Jet Propulsion Laboratory, California Institute of Technology, Pasadena, California, USA.
[2]Scripps Institution of Oceanography, La Jolla, California, USA.

Corresponding author: J.-H. Moon, Jet Propulsion Laboratory, California Institute of Technology, Pasadena, CA, USA. (Jae-Hong.Moon@jpl.nasa.gov)
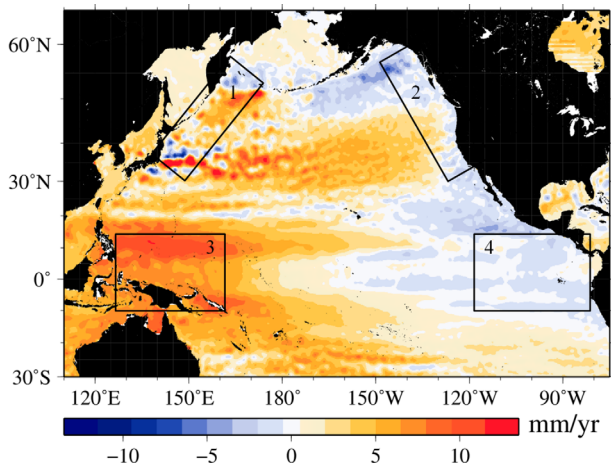
Figure 1. Sea level trends over the Pacific derived from altimetry from 1993 to 2010. Four selected regions, (1) the western boundary of North Pacific, (2) Pacific coast of North America, (3) western tropical Pacific, and (4) eastern tropical Pacific, indicate the areas where the time series of regional mean sea level will be examined.

by a rising trend in the WTP and a declining trend in the ETP [*Feng et al.*, 2010; *Bromirski et al.*, 2011].

[4] On multidecadal time scales, Pacific SLR fluctuations with large spatial and temporal deviations can potentially threaten to inundate low-lying Pacific islands and heavily populated U.S. and Asian coastal regions. Because of the potential negative impact on coastal communities, it is important to understand and quantify the multidecadal SLR trends and their spatial patterns when assessing and projecting the future SLR impacts. As aforementioned, however, many previous studies on long-term sea level variability have relied on sparsely distributed tide gauge records because of the relatively short satellite altimeter record (i.e., since 1993). While tide gauges provide longer records, their spatial resolution is not sufficient to resolve large-scale patterns of ocean fluctuations. Accordingly, less attention has given to the spatial and temporal variability of sea level changes in the Pacific basin prior to the altimetry period, which is the main issue of this paper.

[5] Recently, several attempts have been made to combine these two data sets, i.e., tide gauges and altimeters records, in conjunction with numerical models or reanalysis products, to reconstruct the historical sea levels since the 1950s. *Chambers et al.* [2002] made one of the first combined data performing an empirical orthogonal function (EOF) reconstruction. *Church et al.* [2004] produced the most comprehensive and widely cited sea level reconstruction to date from 1950 to 2001. Since then, other studies on sea level reconstructions used different data sources or methods [e.g., *Llovel et al.*, 2009; *Hamlington et al.* 2011; *Meyssignac et al.*, 2012a]. These long-term reconstructed sea levels with near-global coverage can be valuable resources for studies on the spatial and temporal variability on multidecadal time scales, including projections. In addition to long-term sea level reconstructions, an ocean general circulation model (OGCM) based on a physical framework can serve as a useful tool in quantifying the sea level variations prior to the altimetry era and projecting

long-term SLR trends [*Gregory et al.*, 2004; *Wunsch et al.*, 2007]. So far, most of ocean models are designed to conserve volume applying the Boussinesq approximation, instead of water mass. However, the Boussinesq ocean models may not accurately represent thermosteric effects and ocean bottom pressure (OBP) [*Greatbatch*, 1994; *Ponte*, 1999; *Greatbatch and Lu*, 2001], which are main contributors to sea level changes. Although a globally uniform and time-dependent correction can be effective in computing the GMSL in Boussinesq models, it does not necessarily work in representing regional sea level changes. Recent studies have also discussed the non-Boussinesq effects that allow for a better representation of thermal expansion [*DeSzoeke and Samelson*, 2002; *Song and Hou*, 2006].

[6] In this paper, we characterize and quantify the large-scale multidecadal rSLR and related ocean heat content (OHC) fluctuations in the Pacific using different observational data sets and a non-Boussinesq OGCM, which allows sea level to rise as a direct response to ocean heating. Four data sets are analyzed here: the altimetry-based sea surface height (SSH), two versions of 2-D past sea level reconstructions, and in situ-derived steric sea level (SSL) and OHC. The contributions of steric variations and related surface wind forcing to the regional sea level changes are determined from model simulations, including a sensitivity experiment. Comparing observational data products with the non-Boussinesq model simulation allows us to gain insight into the evolution of spatial pattern of sea level trends in the Pacific over longer time scales, as well as the accuracy and reliability of observed sea level fluctuations.

2. Observational Data Sets and a Non-Boussinesq Model

2.1. Sea Level Data

[7] Altimetry-based sea level observations since 1993 are used to estimate recent SLR tends. Altimetry SSH over 1993–2010 used is a merged product of several altimeter missions (TOPEX/Poseidon, Jason-1, ERS-1, EVISAT). The SSH data were produced and distributed by AVISO (http://www.aviso.oceanobs.com/) as part of the Ssalto ground processing segment. In addition to the altimetry SSH, two recent sea level reconstructions over 1958–2008 are used to examine the SLR trend patterns prior to the altimetry period: (1) *Hamlington et al.* [2011] and (2) *Meyssignac et al.* [2012a] (hereafter H2011 and M2012, respectively).

[8] H2011 presented a new method for reconstructing sea level involving cyclo-stationary empirical orthogonal functions (CSEOF), using both the tide gauge records for the period 1950–2009 and the satellite altimetry records during 1992–2009. Using least squares fitting of the altimeter-derived CSEOF basis functions to the tide gauge data, H2011 produced a sea level reconstruction with global coverage over the period of June 1950 to June 2009, and demonstrated the reliability of the CSEOF-based reconstruction for climate monitoring when focusing on climate signals like ENSO. The detailed descriptions of the reconstruction technique and the computation of the CSEOF are found in H2011 and *Kim at al*. [1996]. The other sea level reconstruction used here is from M2012,

which is based on the technique developed by *Llovel et al.* [2009]. This reconstruction provides an annual time series of global sea level from January 1950 to December 2009. The method consists of first performing an EOF decomposition of 2-D sea level fields based on the output of the DRAKKAR/NEMO OGCM [*Penduff et al.*, 2010], the SODA ocean reanalysis [*Carton and Giese*, 2008], and altimetry-based sea level observations, and then computing new principal components over a longer period covered by tide gauge records and constraining them with a least squares optimal interpolation. Interested readers are referred to M2012 for details on the reconstruction process. The M2012's reconstruction has been validated by comparison with independent tide gauge records not used in the reconstruction process [M2012; *Becker et al.*, 2012].

[9] Because thermal steric expansion associated with changing in temperature structure is the most important cause for the sea level changes and their regional differences, we also examine SSL and OHC derived from in situ upper-ocean (0–700 m) profiles of *Ishii and Kimoto* [2009], which has been produced by objective analysis of observations and consists of monthly gridded temperature and salinity with a 1° spatial resolution from 1945 to 2010. The SSL has been computed at each grid point by integrating the specific volume down to 700 m. We show that considering these data sets together, in terms of multidecadal time scales, is the key to gaining insight into the sea level trends that occurred in the Pacific over the past few decades, as well as for corroborating the accuracy and reliability of observed sea level fluctuations and the reconstructions.

2.2. A Non-Boussinesq OGCM

[10] A non-Boussinesq OGCM, which is an evolving version of ROMS [*Shchepetkin and McWilliams*, 2005], is employed to avoid uncertainties involving the Boussinesq approximations in representing the sea level, its regional trends, and thermal expansion [*DeSzoeke and Samelson*, 2002; *Song and Hou*, 2006; *Song and Colberg*, 2011]. The model has been configured globally with a 1/4° horizontal resolution with 30 terrain-following vertical levels [*Song and Haidvogel*, 1994] and is coupled with a sea ice model [*Budgell*, 2005]. The shallowest and deepest water depths are 20 m and 5500 m, respectively. Both polar regions are included, with the northern pole shifted toward the Russian continent.

[11] The model was initialized with climatological temperature and salinity from the World Ocean Atlas (WOA) 2001, and was spun up for 60 years with National Centers for Environmental Prediction (NECP)/National Center for Atmospheric Research (NCAR) monthly climatology [*Kalnay et al.*, 1996] to reach an approximately steady state. After 60 years spin-up, the model was forced by 6 hourly NCEP/NCAR reanalysis data from 1958 to 2010. The NCEP reanalysis is one of the products most frequently used to force OGCM and has the longest available record length (about 60 year record) compared to other products, which makes it ideal for simulating the long-term fluctuations of the ocean [*McGregor et al.*, 2012]. Surface fluxes of momentum and heat are calculated in ROMS using bulk formulations [*Fairall et al.*, 1996]. No water mass from the land-based water is added to the ocean, but the evaporation minus precipitation distribution is still applied. Thus, the model only estimates internal mass changes that include effects of evaporation and precipitation, conserving the ocean mass changes.

3. Multidecadal Sea Level Trends Over 1958–2008

[12] During the altimetry period of 1993–2010, the most dominant feature of SLR trend is a strong east-west dipole in the tropical Pacific, with positive trends in the WTP and negative trends in the ETP (Figure 1). The strongest rising trend is detected along the band of 8–12°N (>8 mm/yr) in the WTP, in which the mean North Equatorial Current is located. The other noticeable feature is that the SLR trend pattern of variability across the North Pacific basin is similar to the PDO pattern, with strong SLR centered in the western and central North Pacific that is surrounded by the opposite sign SLR along the Pacific coast of North America. These patterns have been previously observed by *Cazenave and Nerem* [2004], who considered the SSH data only over the first decade of the altimetry period (i.e., 1993–2003). This indicates that the SLR patterns have been persistent at least since the early 1990s.

[13] With the two sea level reconstructions and the model results, we can investigate the sea level changes for longer time periods. The time series of annual mean sea level variations over 1958–2008 in four selected regions (see Figure 1) are presented in Figure 2, which shows the model SSH anomalies (red) with the altimeter (green), and the sea level reconstructions of H2011 (black) and M2012 (blue). The GMSL trend, which is significantly influenced by land ice melting that is not included as a model forcing function, has been removed from each of data sets to highlight the regional variability. For all regions, the two sea level reconstructions agree well over the 50 year epoch with high correlations of above 0.7 (correlations are given in Figure 2, statistically significant above the 95% level), and also match the model results, particularly after mid-1970s.

[14] The observed rSLR trends have undergone two shifts, in the mid-1970s and the early 1990s, showing an opposite signal between the western and eastern regions of the Pacific. For the western Pacific (i.e., Regions 1 and 3), there are upward trends of sea level during both periods prior to mid-1970s and after early 1990s, and decreasing or near-stationary trends between 1975 and 1992 (Figures 2a and 2c); in contrast, the eastern Pacific regions (i.e., Regions 2 and 4) are totally out-of-phase with the sea level in the western Pacific (Figures 2b and 2d). Previous studies have pointed out these multidecadal variations in the WTP since the mid-1970s and the early 1990s [e.g., *Feng et al.*, 2010; *Merrifield et al.*, 2012; *Qiu and Chen*, 2012]. A quantitative comparison of the SLR trends among the sea level products in the selected four regions is also shown in Table 1. Similar fluctuations have been also reported by *Meyssignac et al.* [2012b] who have shown that the altimetry-based sea level pattern since the early 1990s is the most frequently observed pattern in the tropical Pacific among successive 17 year trend maps over the last 60 years. The multidecadal rSLR trends are more clearly visible in Figure 3, which shows the spatial patterns of SLR trends in the Pacific over the following three multidecadal
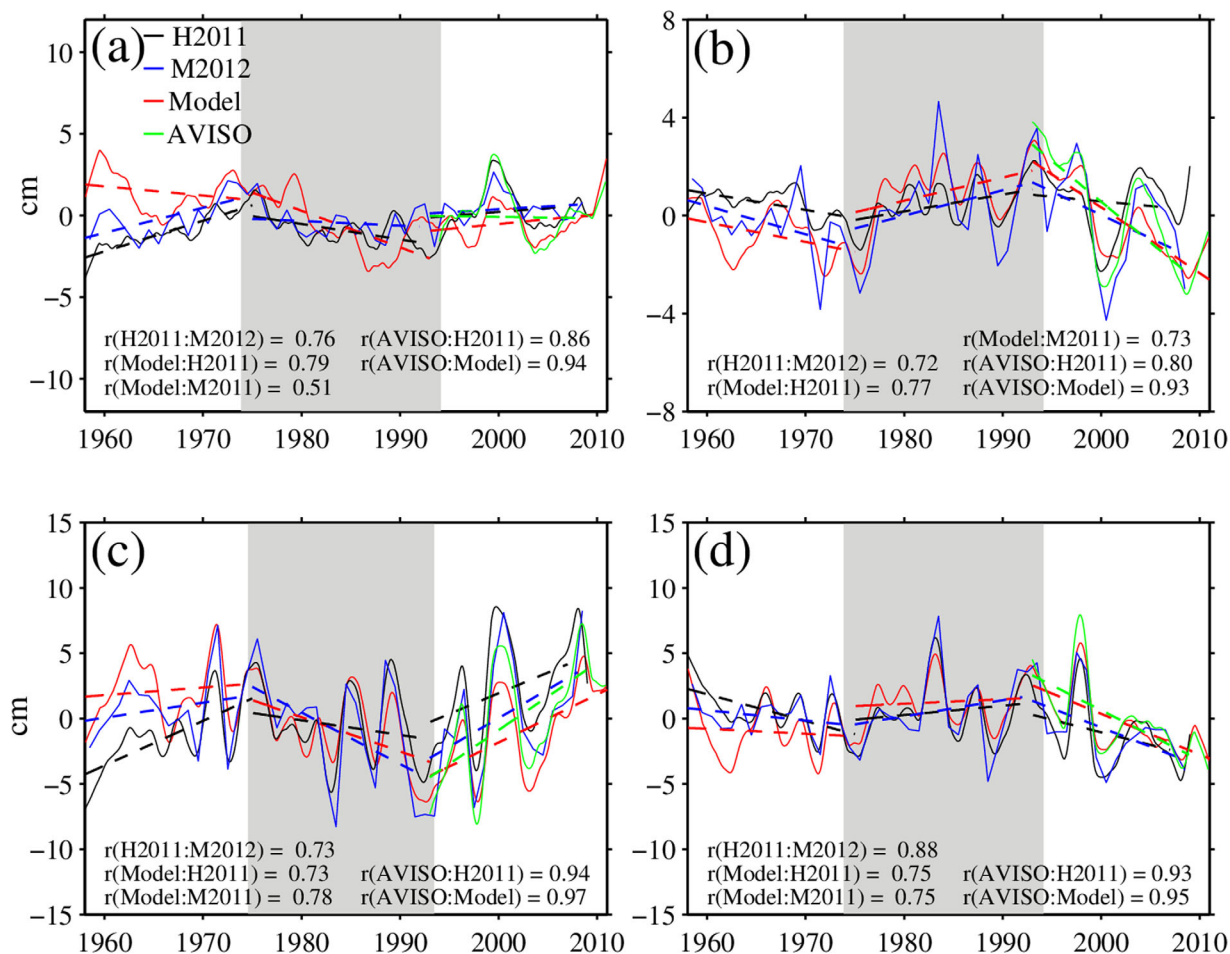
Figure 2. Comparison of model sea level variations (red) with altimeter SSH over 1993–2010 (green), two past sea level reconstructions of H2011 (black) and M2012 (blue) over 1958–2008 over regions defined in Figure 1: (a) the western boundary of North Pacific, (b) Pacific coast of North America, (c) western tropical Pacific, and (d) eastern tropical Pacific. The dashed lines indicate the linear trends for three multidecadal periods divided by shaded region; 1958–1974, 1975–1992, and 1993–2008. The linear correlations are given at the bottom of each plot. The global mean sea level trend in each data set was removed.

periods: period I (1958–1974), period II (1975–1992), and period III (1993–2008). To emphasize the regional variability, the global mean trend has been removed from each of data sets. The two sea level reconstructions and the model display similar spatial patterns, with a strong dipole in the tropics and larger discrepancies in period I (Figures 3a and 3f), which will be discussed later. Nevertheless, the sea level trends over period I are quite similar to those in period III, but are opposite to the pattern in period II (mid-1970s to 1980s), representing a large-scale multidecadal rSLR shift in mid-1970s and early 1990s, respectively. The sea levels have fluctuated on a multidecadal time scale during at least the last 50 years, although the amplitude of their variability is much less than ENSO-related interannual signals.

[15] Compared to observed data sets, our hindcast simulation well reproduces the spatial patterns of observed rSLR trends as well as their time series for each region,

Table 1. Linear (mm/yr) Trends of Altimeters (AVISO), Two Reconstructions (H2011 and M2012), and Model (NB) Sea Levels in Defined Four Regions in Figure 1 During the Three Multidecadal Period: (I) 1958–1974, (II) 1975–1992, and (II) 1993–2008[a]

	Region 1				Region 2				Region 3				Region 4			
Periods	H2011	M2012	NB	AVISO	H2011	M2012	NB	AVISO	H2011	M2012	NB	AVISO	H2011	M2012	NB	AVISO
I	1.7	1.6	−0.5	–	−0.7	−1.0	−0.8	–	3.5	1.1	0.8	–	−1.7	−1.1	−0.6	–
II	−0.9	−0.4	−1.4	–	0.7	0.9	0.9	–	−1.1	−3.7	−2.6	–	0.8	1.1	0.4	–
III	0.4	0.3	0.5	0.2	−1.1	−2.5	−3.0	−3.2	3.6	4.5	4.2	5.1	−2.4	−3.1	−3.5	−3.8

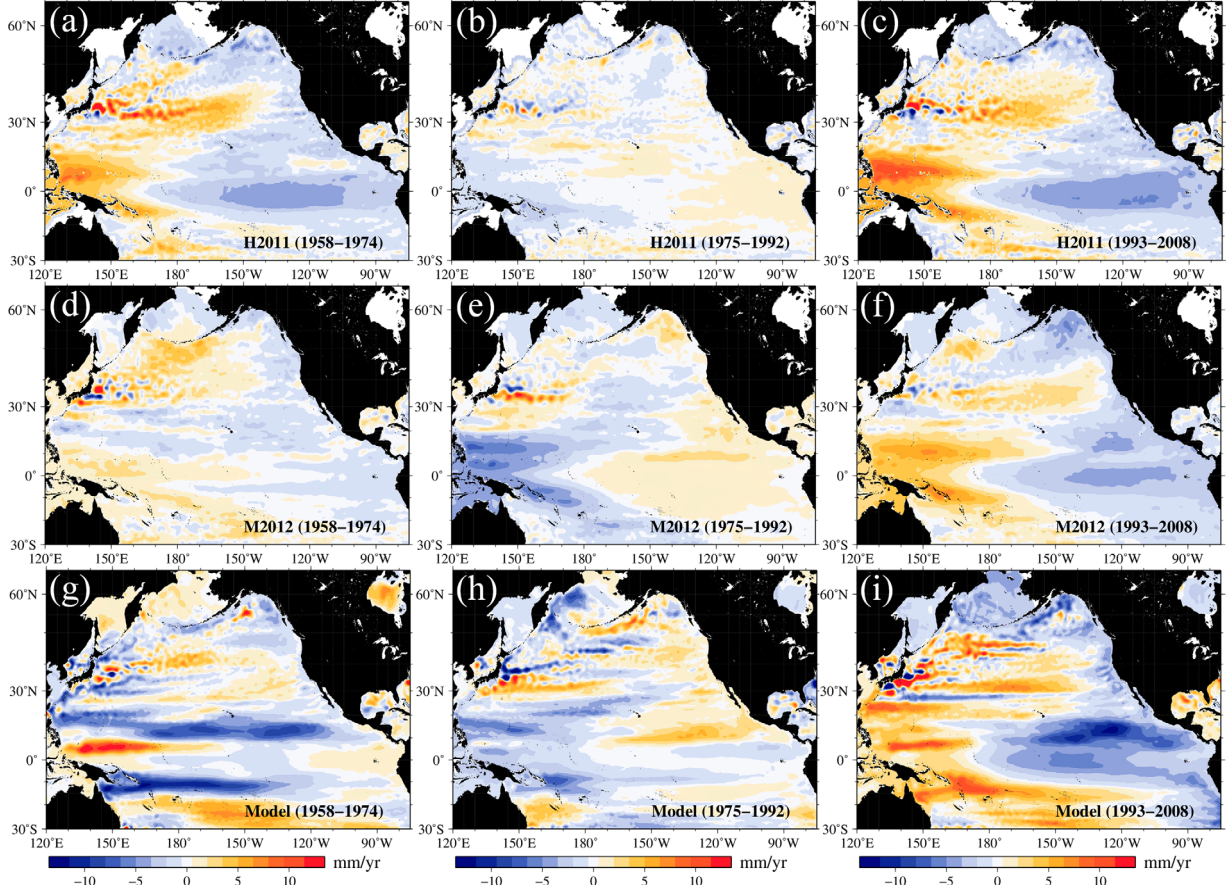[a]The global mean sea level trend in each data set was removed.

4

Figure 3. Sea level trends over the Pacific derived from two sea level reconstructions of (top, a–c) H2011, (middle, d–f) M2012, and (bottom, g–i) model over three multidecadal periods. The global mean sea level trend in each data set was removed.

except for a discrepancy during the period I, particularly for the western Pacific regions (Figure 3g). The discrepancy during the first period may be caused by uncertainties from the initial condition—a result of 60 year spin-up with climatological forcing that might not be ideal for the early period of simulation, or uncertainties in the wind stress forcing, which are magnified when computing gradients associated with wind stress curl. *McGregor et al.* [2012] reported differences between the observed SLR trend in the WTP and a 1.5-layer shallow water model driven by NCEP wind forcing, suggesting significant uncertainties in the NCEP wind product, particularly prior to 1970s. Meanwhile, *Nidheesh et al.* [2012] also showed that the NCEP wind trend in the Pacific tropical region after 1970s has a good agreement with other wind products like ERA40 and WASWind. Thus, the uncertainty in the NCEP wind trend during the first period may be one of the causes of the discrepancy between the reconstructed SLR trends and our modeled SLR trends in the western Pacific regions. On the other hand, the reconstructed sea levels for the period I may also have larger uncertainties, suggested by the difference between the two reconstructed products. Nevertheless, the multidecadal rSLR shifts with a PDO-like spatial structure are well reproduced by the simulation after mid-1970s.

4. Steric and Nonsteric Contributions to the Multidecadal Sea Level Trends

[16] Based on the sea level budget closure, rSLR should match the sum of SSL and ocean mass changes:

$$SL = SL_{steric} + SL_{mass} \tag{1}$$

where

$$SL_{steric} = \frac{1}{\rho_0} \int_{-H}^{0} \frac{\partial \rho}{\partial t} dz \tag{2}$$

$$SL_{mass} = \frac{1}{g\rho_0} \frac{\partial P_b}{\partial t} \tag{3}$$

[17] Here SL_{steric} and SL_{mass} represent density (temperature and salinity) changes of the water column and those associated with net mass changes of the water column, respectively. P_b is OBP, ρ ocean density, ρ_0 a reference density, g gravity coefficient, and H ocean depth. The contributions of the two components to rSLR can be determined from our mass-conserving OGCM. Figure 4 shows the upper-ocean (0–700 m) SSL trends derived from *Ishii and Kimoto* [2009] (top) and model (middle), and model
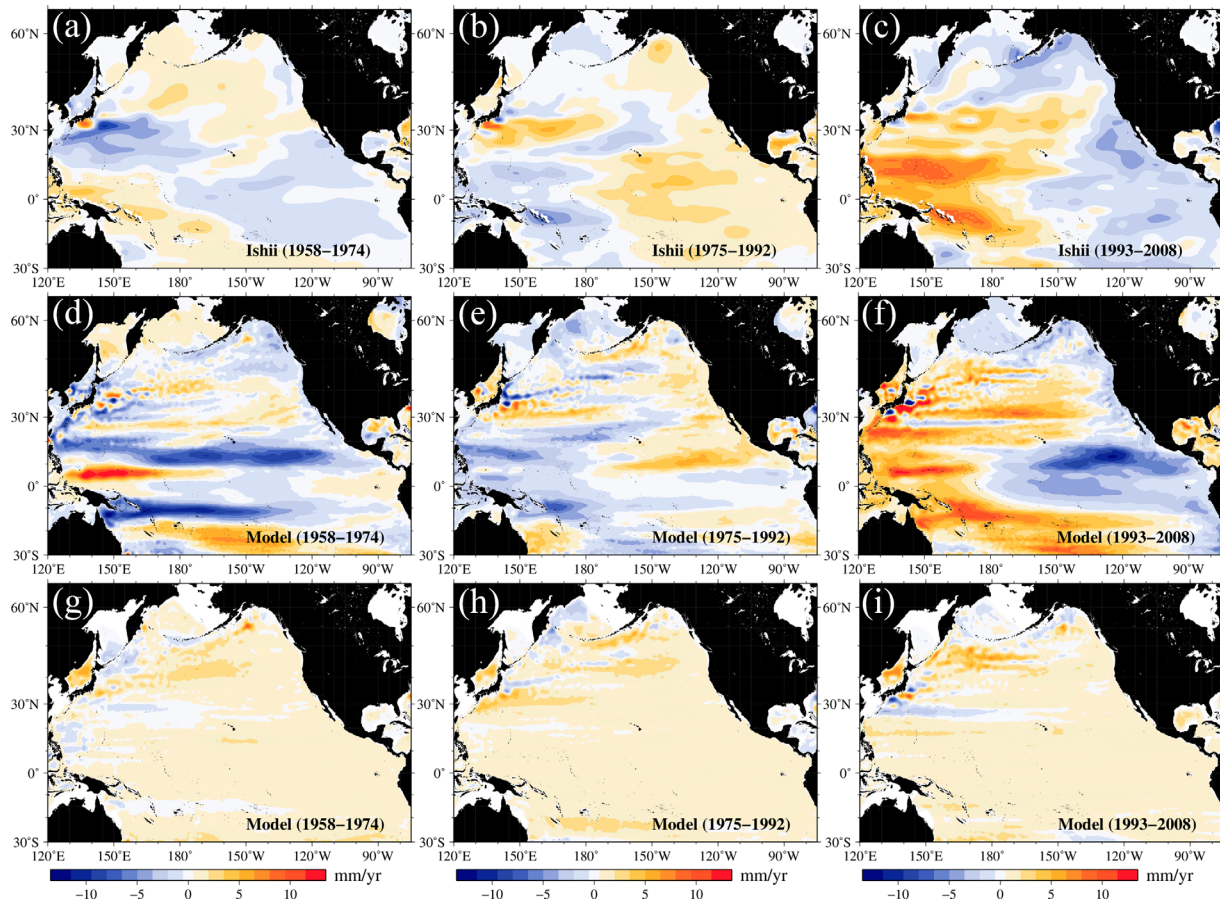
Figure 4. (top) Steric sea level (SSL) trends over the Pacific derived from in situ measurements of *Ishii and Kimoto* [2009], (middle) model upper-700 m, and (bottom) model ocean bottom pressure (OBP) trend over three multidecadal periods.

OBP trend (bottom) over the three multidecadal periods. The observed SSL trends have similar multidecadal patterns to those of sea level, emphasizing a close correspondence between regional sea level and upper-ocean SSL variability; i.e., trends of period I are similar to those of the period III, but opposite during the period II (mid-1970s and 1980s). This large-scale pattern is also well reproduced by our model except for the period I which may be due to several sources of uncertainty, such as from the initial condition and wind product, as mentioned above, indicating that SSL variation is substantially determined by the changes in the upper ocean. On the other hand, mass-induced variation derived from the model OBP (i.e., $P_b/g\rho_0$ is the same dimension as SSH in meters) contributes little to the sea level trend on the multidecadal time scale (Figure 4, bottom). It indicates that the rSLR trend can be largely explained by steric effect due to density changes, including surface heat from the atmosphere locally and heat redistribution by ocean dynamics, as opposed to depth-integrated ocean mass variations.

[18] The SSL change includes both thermosteric and halosteric changes, but is mainly dominated by thermosteric (thermal expansion) changes [e.g., *Antonov et al.*, 2005; *Domingues et al.*, 2008]. The time series of model upper (0–700 m, red) OHC in the defined four regions are shown in the Figure 5 (left), and are compared with in situ upper

OHC (black lines) from *Ishii and Kimoto* [2009]. The model results are fairly consistent with in situ measurements in the multidecadal trends as well as in their interannual variations, which confirms the close correspondence between the rSLR and thermal (temperature) change in all regions. About 80% of the OHC trends in these regions can be explained by the changes in the upper-700 m OHC. It is shown that changes in the OHC are able to account for most of the observed sea level changes [*Auad et al.*, 1998; *Kelly*, 2004]. Moreover, the regional OHC change (Q_t) in the ocean can be further divided into two contributions: regional surface (air-sea) heat fluxes (Q_{net}) and lateral heat transport associated with convergence and divergence of oceanic heat (Q_{adv}), i.e., $Q_t = Q_{net} + Q_{adv}$. The contributions to the OHC changes can be elucidated by the time series of each component obtained from the model output (Figure 5, right). Vertically integrated temperature flux for the entire water column is used to calculate the convergence/divergence of horizontal temperature flux in and out of the regions. After removing seasonal variability, the OHC changes are strongly correlated with the oceanic heat advection: above 0.7 for all regions, but poorly correlated with the surface net fluxes: below 0.3 for all regions. This shows that the temporal changes of OHC are mainly dominated by the effect of horizontal convergence/divergence of temperature in and out of the regions, particularly more in
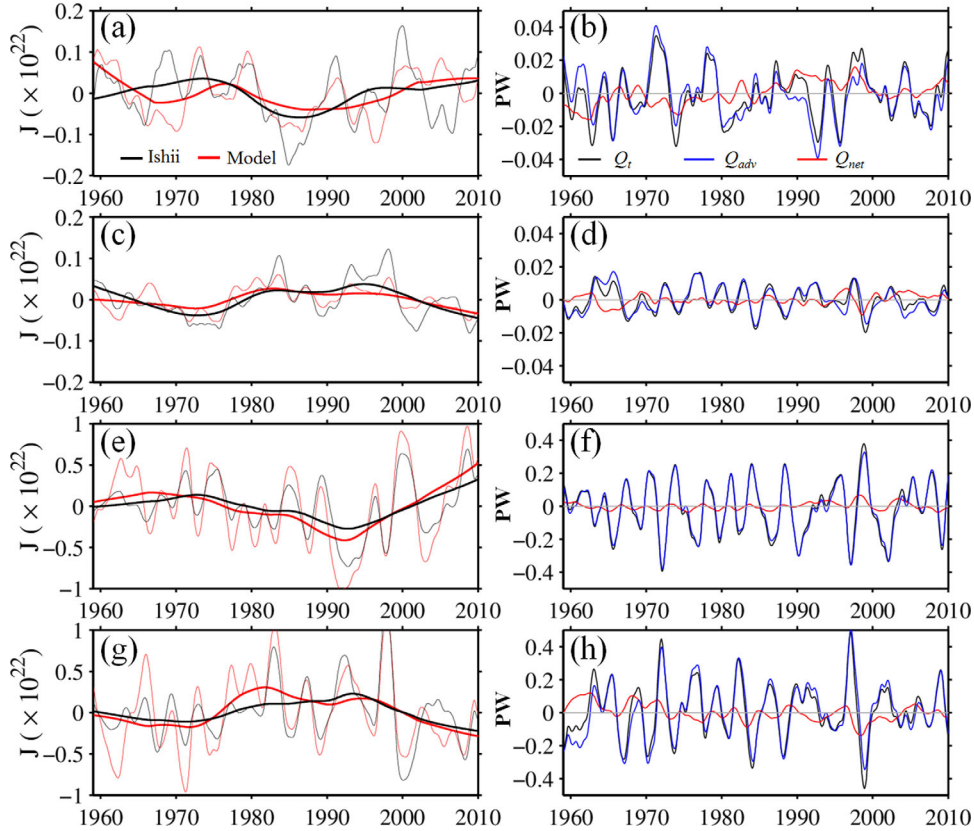
Figure 5. Time series of in situ upper-700 m ocean heat content (OHC, black), (red, left) corresponding model upper OHC and (right) oceanic heat balance after removing seasonal cycle time-varying OHC (Q_t), heat advection (Q_{adv}), and surface heat fluxes (Q_{net}), over 1958–2008 over regions defined in Figure 1: (a and b) the western boundary of North Pacific, (c and d) Pacific coast of North America, (e and f) western tropical Pacific, and (g and h) eastern tropical Pacific. The thick lines in left plots indicate low-pass (18 year) filtered values.

the tropical regions. This is consistent with the previous observational and model studies [*Auad et al*., 1998; *Dong and Kelly*, 2004; *Moon and Song*, 2013], confirming that surface heat fluxes contribute more to the heat changes on the seasonal timesscale, whereas the heat redistribution due to ocean circulation contributes more on the longer time scales. The model-data analysis in sea level relation suggests that on multidecadal time scale, steric changes associated with lateral heat transport by ocean circulation dominate the rSLR, with negligible contribution from internal mass changes of ocean.

5. Sea Level Trend Shifts Associated the PDO

[19] To focus on the relationship between the rSLR and the Pacific climate variability on multidecadal time scales, we compared low-pass filtered (18 year) sea level reconstructions after removing their GMSL rates, with the PDO index from the Joint Institute for the Study of the Atmosphere and Ocean (JISAO; http://jisao.washington.edu/) (Figure 6). The PDO index (green lines in Figure 6) shows trend changes in the early 1970s and 1990s that are related to multidecadal variations in the Pacific climate modes. The rSLR trends in all regions are shifted twice in line with the climate index. In the western Pacific (Figures 6a

and 6c), two reconstructed sea levels show a rising trend during both periods of I and III, i.e., prior to the mid-1970s and after early 1990s when the PDO index is in a declining trend; on the other hand, they fall during the period II (mid-1970s and 1980s) when the index is in a rising trend. This indicates that there is significant negative correlation between the western Pacific sea levels and the PDO index; e.g., correlations between the 5 year filtered WTP sea level and the PDO over the 1958–2008 are −0.62 and −0.60 for the H2011 and the M2012 (statistically significant above the 95% level), respectively. The negative correlations with the PDO were also identified by *Merrifield et al*. [2012] who focused on the multidecadal WTP sea level changes. The model is also shown to be quite consistent with the sea level reconstructions, showing a significant correlation of −0.65 with the PDO index (statistically significant above the 95% level).

[20] In contrast, the sea levels in the eastern Pacific fluctuate on the multidecadal time scales, but in opposite phase to the western Pacific regions, with a positive correlation with the PDO index (Figures 6b and 6d). It is important to note that over the recent two decades the rSLR trends of the eastern Pacific associated with climate variability have a declining trend, while the GMSL trend due to global warming accelerated during the same period. The
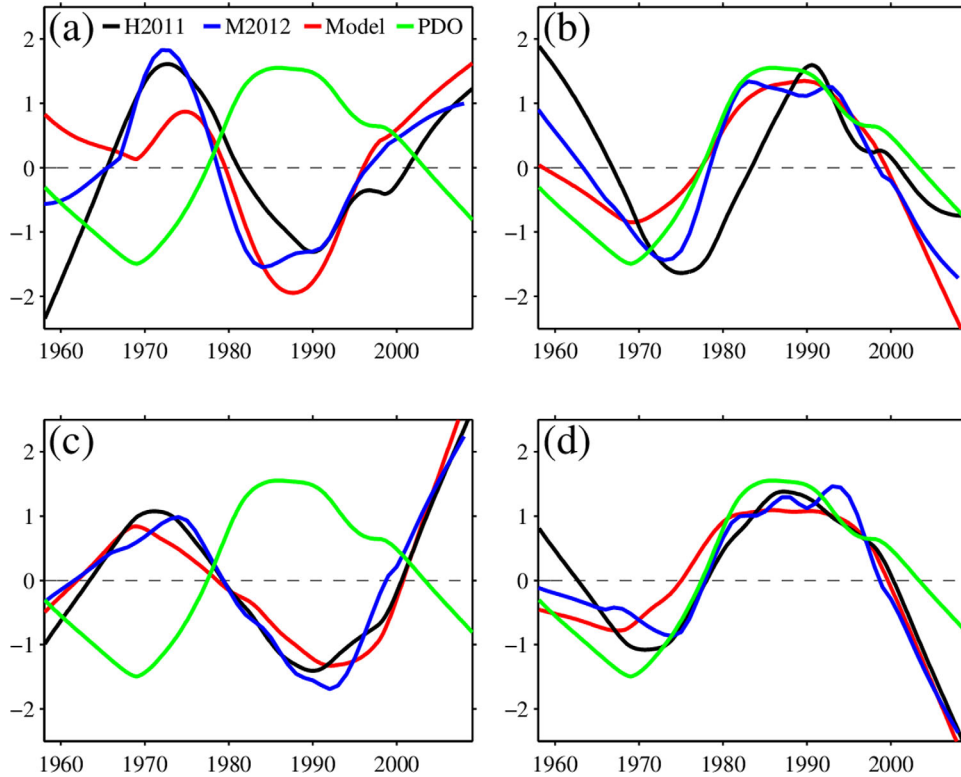
Figure 6. Comparison of long-term sea level variations from model (red) and two reconstructions of H2011 (black) and M2012 (blue) with the Pacific Decadal Oscillation (PDO) index (green) over regions defined in Figure 1: (a) the western boundary of North Pacific, (b) Pacific coast of North America, (c) western tropical Pacific, and (d) eastern tropical Pacific. All values were low-pass filtered (18 year) and normalized by their respective standard deviation.

multidecadal trend associated with the Pacific climate variability contributes to the suppression of rSLR in the eastern Pacific over the past two decades, which has been noted by *Bromirski et al.* [2011] who focused on the relationship between the rSLR along the Pacific coast of North America and the PDO. The large-scale relationship between Pacific sea level and climate variability is illustrated by spatial correlation maps (Figure 7). The sea levels in the WTP and the western/central North Pacific (i.e., region of south the Aleutians) anticorrelate with those of the ETP and the Pacific coast of North America, identifying an association of the Pacific sea levels with climate-forced large-scale patterns. It is worth noting that the sea level changes in the Kuroshio Extension region, where relatively weak positive correlations are shown, may be associated with westward Rossby waves that propagate signals from the eastern/central Pacific into the KE regions [e.g., *Schneider and Miller*, 2001; *Qiu*, 2003; *Taguchi et al.* 2007; *Di Lorenzo et al.* 2008]. Our OGCM is well capturing the dominant climate mode of rSLR changes, showing the model capacity to reproduce the observed Pacific sea level patterns.

6. Sea Level Shifts and PDO-Related Wind Forcing

[21] Surface wind forcing that dynamically drives the upper-ocean circulation can be an important contributor for regional sea level variability and long-term trends [e.g.,

Lee and McPhaden, 2008; *Timmermann et al.*, 2010]. To assess the surface wind patterns associated with the Pacific climate variability, we have projected the wind stress patterns in the Pacific upon the PDO index by a multiple linear regression approach (Figure 8a). The regression coefficients for the PDO index are strong in the Pacific trade wind region and approximately north of 30°N (i.e., Aleutian low region), showing consistency with *Merrifield et al.* [2012]. These PDO-related wind patterns probably contribute to sea level responses that match the negative and positive correlations between the sea levels and the PDO in the western and eastern Pacific, respectively (see Figure 7).

[22] The multidecadal rSLR responses to surface wind variability are evident in time series of regionally averaged wind stress curl in the North Pacific (140°E–130°W, 30°N–60°N, Figure 8b) and averaged zonal wind stress in the tropical Pacific (140°E–100°W, 15°S–15°N, Figure 8c). The easterly trade wind across the tropical Pacific and negative wind stress curl in the North Pacific (north of 30°N) tend to intensify from the early 1990s onward (period III). The wind trends prior to mid-1970s (period I) is slightly different in strength, but indicates intensified trades in the tropic and negative wind stress curl in the North Pacific, implying that the recent surface wind trends may have existed prior to the mid-1970s. On the other hand, the wind trend between 1975 and 1992 (period II) shows an opposite trend of the easterly trade in the tropic and wind stress curl in the North Pacific. The multidecadally modulating surface
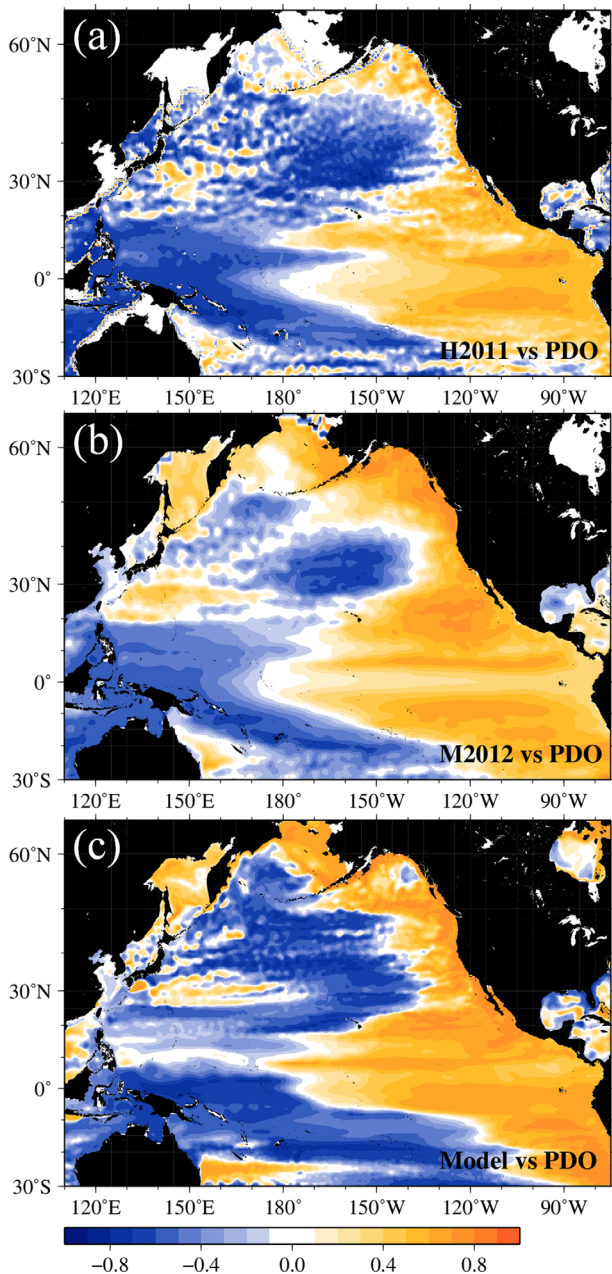
Figure 7. Correlations of 5 year running mean PDO index with (a) H2011's sea level reconstruction, (b) M2012's sea level reconstruction, and (c) model sea level over 1958–2008.

were captured in many reanalysis wind products, although they are different in spatial shape and magnitude [*Feng et al.*, 2011; *Nidheesh et al.*, 2012]. Similarly, the multidecadal wind stress curl changes in the North Pacific can contribute to regional sea level variability in the western/central North Pacific and along the Pacific coast of North America owing to the broad-scale convergences and divergences induced by Ekman dynamics; e.g., declining SLR trends along the west coast of North America are associated with the strengthened negative wind stress curl prior to mid-1970s and after early 1990s, while an opposite sense occurs during the second period (from mid-1970s to early 1990s).

[23] A sensitivity experiment using only wind trend changes allows ascertaining the dynamical response of long-term regional sea level fluctuations to large-scale surface wind forcing, which is what we focused previously. Similar to the experiment of *Moon and Song* [2013], we computed a sensitivity experiment (named Wcase) with detrended NCEP wind stress fluctuations over the entire Pacific during the period III (1993–2008). Without the recent wind stress trend, the modeled sea level shows quite different spatial trends from the baseline (original run); the model no longer reproduces the large-scale PDO-like structure (not shown). The sea level trends during the period III are significantly weakened (strengthened) in the western
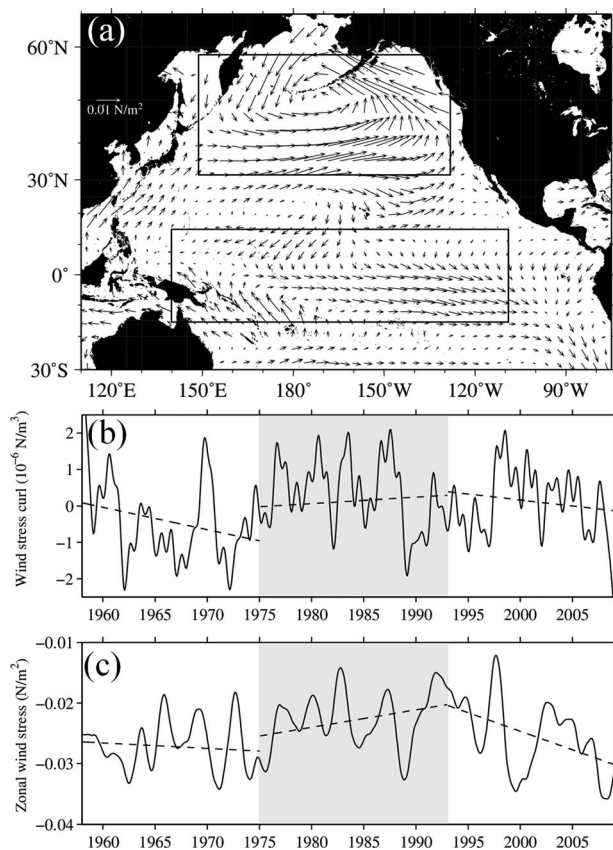

Figure 8. (a) NCEP wind stress regressed on the PDO index in a multiple linear regression. (b) Time series of Figure 8a mean wind stress curl over the North Pacific and (c) zonal wind stress in the tropical Pacific (boxed regions in Figure 7a). The dashed lines indicate linear trends over three multidecadal periods.
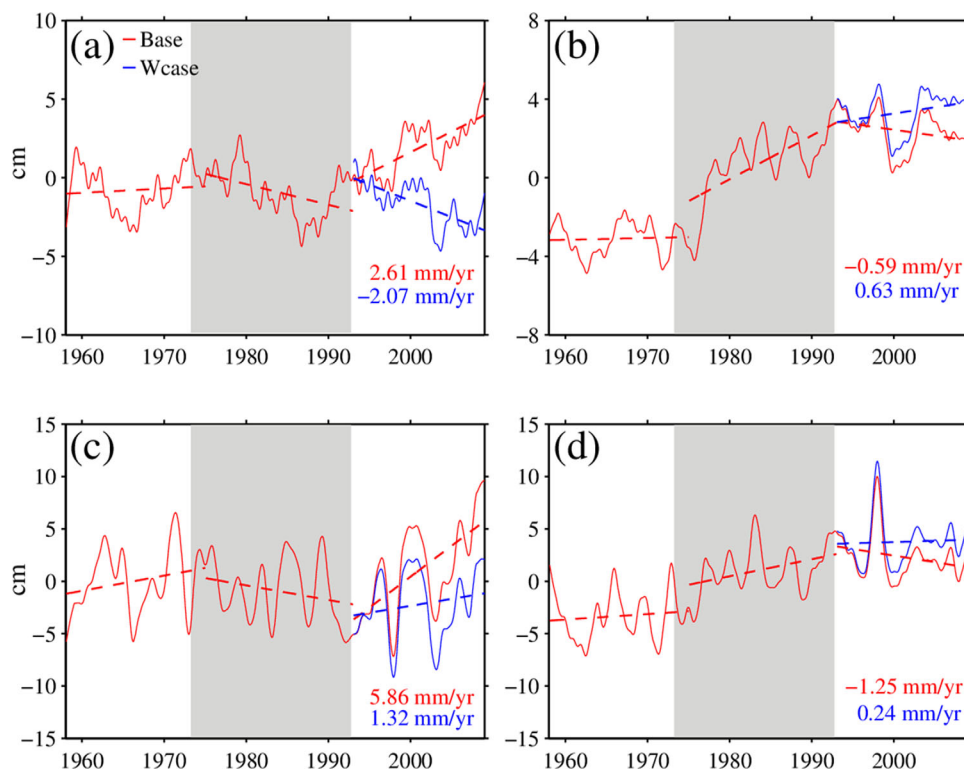
wind forcing matches well with the sea level changes in the Pacific. During both periods prior to mid-1970s and after early 1990s, the enhanced easterly Pacific trade wind (-1.7×10^{-4} and -4.2×10^{-4} N/m^2/yr for the periods I and III, respectively) contributes to high (low) WTP (ETP) sea level due to a balance between the wind stress and zonal sea level gradients [e.g., *Timmermann et al.*, 2010; *Feng* et al., 2011; *Qiu and Chen*, 2012]. However, the WTP (ETP) sea level trend has a decreasing (increasing) trend between the mid-1970s and early 1990s, corresponding to the weakening trend in the trade winds across the tropical Pacific with a rate of 2.7×10^{-4} N/m^2/yr. These multidecadal wind trends

Figure 9. Comparison of sea level variation between the baseline (red) and the Wcase (blue lines) over the 1993–2008 over regions defined in Figure 1: (a) the western boundary of North Pacific, (b) Pacific coast of North America, (c) western tropical Pacific, and (d) eastern tropical Pacific. The dashed lines indicate the linear trends, with their rates during 1993–2008.

(eastern) Pacific regions compared to those of the baseline. The upward trends in the western Pacific are much slower (or even decreased) in the Wcase (−2.07 and 1.32 mm/yr) than those of the baseline (2.61 and 5.86 mm/yr at the Regions 1 and 3, respectively) (Figures 9a and 9c). In contrast, the eastern Pacific shows opposite sea level trend responses to those of the western Pacific regions (Figures 9b and 9d). This confirms that wind stress changes associated with the Pacific climate mode during the period 1993–2008 played an important role in strengthening the rSLR in the western Pacific while suppressing the rSLR in the eastern Pacific, resulting in the changes of SSL due to a convergence/divergence in the upper ocean.

7. Summary and Discussion

[24] Previous studies based on altimetry and sparse tide gauge data have shown great regional sea level differences and various types of low-frequency variations in the Pacific [e.g., *Feng et al.*, 2004; *Bromirski et al.* 2011; *Khöl and Stammer*, 2008; *Meyssignac et al.*, 2012b]. Here we show how the Pacific sea levels have changed spatially and temporally on the multidecadal scale in a unified manner, and explain the dynamics associated with climate variability. To gain insight into the long-term sea level changes in the Pacific over 1958–2008, we first characterized the multidecadal rSLR trends and their spatial pattern in the Pacific using altimetry-based sea level, reconstructed sea levels of H2011 and M2012, in situ upper-ocean profiles, and results

from a non-Boussinesq OGCM. The model is used to explain the dynamics where no observational data are available. We then focused on the contributions of steric variations and related surface wind forcing to the regional sea level changes through analyzing model output results.

[25] Over the altimetry period, the SLR trend shows a large-scale PDO-like structure that exhibits a strong east-west dipole pattern in the tropics and a high positive sea level anomaly in the western/central North Pacific with low anomalies along the Pacific coast of North America. Using the past sea level reconstructions (1958–2008), we found that the sea level trend has fluctuated in the past with multidecadal time scale and showed strong regional differences. While the 1958–1974 rSLR trends are quite similar to those of the 1993–2008, an opposite pattern occurred between those multidecadal periods, i.e., from the mid-1970s to the 1980s. Because the sea level has two components, the steric component due to heat expansion and the nonsteric component due to mass change, we used the upper OHC data and the model to separate their contributions. It is shown that the multidecadal rSLR shifts in the Pacific are the consequence of upper-ocean heat changes due to ocean circulations, with negligible contributions from the depth-integrated ocean mass variations.

[26] To confirm that the multidecadal ocean heat shifts in the Pacific are of climate variability origin, we compared the regional sea levels with the PDO index, showing that they are well correlated with the PDO with a negative correlation in the WTP and the western/central North Pacific

and a positive correlation in the ETP and the Pacific coast of North America. Analyzing wind patterns shows that low-frequency wind patterns can maintain the multidecadal upper-ocean heat changes in the Pacific. The PDO-related changes in tropical trade winds and North Pacific wind stress curl cause strong regional differences of sea levels and drive the long-term sea level fluctuations, balancing the convergences and divergences induced by the Ekman dynamics. Such a mechanism is demonstrated by comparing modeling results with and without the low-frequency wind, indicating the important role played by basin-scale ocean circulation associated with the Pacific climate variability in redistributing heat in the regional Pacific Ocean. In particular, the downward trend in sea level along the U.S. West coast since 1990 is flipped into an upward trend if the basin-wide trends in wind stress curl forcing are removed. This demonstrates the sensitivity of the regional results to the details of the basin-wide wind stress products used to compute the required gradients, which may have considerable error due to limited observations constraining the atmospheric analyses of past decades.

[27] The long-term data analysis and model experiments have implications for projecting future rSLR variations. For example, as pointed out by *Bromirski et al.* [2011], if the multidecadal surface wind pattern fluctuates persistently, associated shifts with the Pacific climate mode may result in promoting rSLR in the ETP and along the eastern boundary of North Pacific over the post-20 year time scale. Changes in dominant large-scale mode patterns, such the recent tendency for the North Pacific Gyre Oscillation [*Di Lorenzo et al.*, 2008] to become more energetic and persistent, also need to be studied in this sea level trend context. With regard to the impact of the multidecadal rSLR on the coastal communities, its superposition over the GMSL due to anthropogenic forcing would certainly enhance the threat to inundate low-lying Pacific islands and heavily populated coastal regions, including the U.S. West coast and Asian coast. In addition, the demonstration of the model capability in capturing the dominant climate mode of sea level and related OHC changes suggests the potential for better projecting and understanding of future evolutions of rSLR.

References

Antonov, J. I., S. Levitus, and T. P. Boyer (2005), Thermosteric sea level rise, 1955–2003, *Geophys. Res. Lett.*, *32*, L12602, doi:1029/2005GL023112.

Auad, G., A. J. Miller, and W. B. White (1998), Simulation of heat storages and associated heat budgets in the Pacific Ocean. 2: Interdecadal timescale, *J. Geophys. Res.*, *103*, 27,621–27,636.

Becker, M., B. Meyssignac, W. Llovel, A. Cazenave, and T. Delcroix (2012), Sea level variations at Tropical Pacific Islands during 1950–2009, *Global Planet. Change*, *80/81*, 85–98.

Bromirski, P. D., A. J. Miller, R. E. Flick, and G. Auad (2011), Dynamical suppression of sea level rise along the Pacific coast of North America:

Indications for imminent acceleration, *J. Geophys. Res.*, *116*, C07005, doi:10.1029/2010JC006759.

Budgell, W. P. (2005), Numerical simulation of ice-ocean variability in the Barents Sea region, *Ocean Dyn.*, *55*, 370–387, doi:10.1007/s10236-005-0008-3.

Carton, J., and B. Giese (2008), A reanalysis of ocean climate using Simple Ocean Data Assimilation (SODA), *Mon. Weather Rev.*, *136*, 2999–3017.

Cazenave, A., and R. S. Nerem (2004), Present-day sea level change: Observations and causes, *Rev. Geophys.*, *42*, RG3001, doi:10.1029/2003RG000139.

Chambers, D. P., C. A. Melhaff, T. J. Urban, D. Fuji, and R. S. Nerem (2002), Low-frequency variations in global mean sea level: 1950–2000, *J. Geophys. Res.*, *107*(C4), 3026, doi:10.1029/2001JC001089.

Church, J. A., N. J. White, R. Coleman, K. Lambeck, and J. K. Mitrovica (2004), Estimates of the regional distribution of sea level rise over the 1950–2000 period, *J. Clim.*, *17*, 2609–2625.

Church, J. A., P. L. Woodworth, T. Aarup, and W. S. Wilson (Eds.) (2010), *Understanding Sea-Level Rise and Variability*, Wiley-Blackwell, Hoboken, N. J.

De Szoeke, R. A. and R. M. Samelson (2002), The duality between the Boussinesq and non-Boussinesq hydrostatic equations of motion, *J. Phys. Oceanogr.*, *23*, 2194–2203.

Di Lorenzo, E., et al. (2008), North Pacific Gyre Oscillation links ocean climate and ecosystem change, *Geophys. Res. Lett.*, *35*, L08607, doi:10.1029/2007GL032838.

Domingues, C. M., J. A. Church, N. J. White, P. J. Gleckler, S. E. Wijffels, P. M. Barker, and J. R. Dunn (2008), Improved estimates of upper-ocean warming and multi-decadal sea-level rise, *Nature*, *453*, 1090–1093, doi:10.1038/nature07080.

Dong, S., and K. A. Kelly (2004), Heat budget in the Gulf Stream region: The importance of heat storage and advection, *J. Phys. Oceanogr.*, *34*, 1214–1231.

Fairall, C. W., E. F. Bradley, D. P. Rogers, J. B. Edson, and G. S. Young (1996a), Bulk parameterization of air-sea fluxes for tropical ocean-global atmosphere coupled-ocean atmosphere response experiment, *J. Geophys. Res.*, *101*, 3747–3764, doi:10.1029/95JC03205.

Feng, M., Y. Li, and G. Meyers (2004), Multidecadal variations of Fremantle sea level: Footprint of climate variability in the tropical Pacific, *Geophys. Res. Lett.*, *31*, L16302, doi:10.1029/2004GL019947.

Feng, M., M. J. McPhaden, and T. Lee (2010), Decadal variability of the Pacific subtropical cells and their influence on the southeast Indian Ocean, *Geophys. Res. Lett.*, *37*, L09606, doi:10.1029/2010GL042796.

Feng, M., C. Böning, A. Biastoch, E. Behrens, E. Weller, and Y. Masumoto (2011), The reversal of the multi-decadal trends of the equatorial Pacific easterly wind, and the Indonesian Throughflow and Leeuwin Current transports, *Geophys. Res. Lett.*, *38*, L11604, doi:10.1029/2011GL047291.

Greatbatch, R. J. (1994), A note on the represent of steric sea level in models that conserve volume rather than mass, *J. Geophys. Res.*, *99*, 12,767–12,771, doi:10.1029/94JC00847.

Greatbatch, R. J., and Y. Lu (2001), Relaxing the Boussinesq approximation in ocean circulation models, *J. Atmos. Oceanic Technol.*, *18*, 1911–1923, doi:10.1175/1520-0426(2001)018<1911:RTBAIO>2.0.CO;2.

Gregory, J. M., H. T. Banks, P. A. Stott, J. A. Lowe, and M. D. Palmer (2004), Simulated and observed decadal variability in ocean heat content, *Geophys. Res. Lett.*, *31*, L15312, doi:10.1029/2004GL020258.

Hamlington, B. D., R. R. Leben, R. S. Nerem, W. Han, and K.-Y. Kim. 2011. Reconstruction sea level using cyclostationary empirical orthogonal functions, *J. Geophys. Res.*, *116*, C12015, doi:10.1029/2011JC007529.

Ishii, M., and M. Kimoto (2009), Reevaluation of historical ocean heat content variations with time-varying XBT and MBT depth bias corrections, *J. Oceanogr.*, *65*, 287–299, doi:10.1007/s10872-009-0027-7.

Kalnay, E., et al. (1996), The NCEP/NCAR, 40-year reanalysis project, *Bull. Am. Meteorol. Soc.*, *77*, 437–471, doi:10.1175/1520-0477(1996)077<0437:TNYRP>2.0.CO;2.

Kelly, A. K. (2004), The relationship between oceanic heat transport and surface fluxes in the western North Pacific: 1970–2000, *J. Clim.*, *17*, 573–588, doi:10.1175/1520-0442(2004)017<0573:TRBOHT>2.0.CO;2.

Kim, K.-Y., G. R. North, and J. Huang (1996), EOFs of one-dimensional cyclostationary time series: Computations, examples, and stochastic modeling, *J. Atmos. Sci.*, *53*, 1007–1017, doi:10.1175/1520-0469(1996)053<1007:EOODCT>2.0.CO;2.

Köhl, A., and D. Stammer (2008), Decadal sea level changes in the 50-year GECCO ocean synthesis, *J. Clim.*, *21*, 1876–1889, doi:10.1175/2007JCLI2081.1.

Lee, T., and M. J. McPhaden (2008), Decadal phase change in large-scale sea level and winds in the Indo-Pacific region at the end of the 20th century, *Geophys. Res. Lett.*, *35*, L01605, doi:10.1029/2007GL032419.

Llovel, W., A. Cazenave, P. Rogel, A. Lombard, and M. B. Nguyen (2009), Two-dimensional reconstruction of past sea level (1950–2003) from tide gauge data and an Ocean General Circulation Model, *Clim. Past*, *5*, 217–227.

McGregor, S., A. Sen Gupta, and M. H. England (2012), Constraining wind stress products with sea surface height observations and implications for Pacific Ocean sea level trend attribution, *J. Clim.*, *25*, 8164–8167, doi:10.1175/JCLI-D-12-00105.1.

McPhaden, M. J., and D. Zhang (2002), Slowdown of the meridional overturning circulation in the upper Pacific Ocean, *Nature*, *415*, 603–608.

Merrifield, M. A., P. R. Thompson, and M. Lander (2012), Multidecadal sea level anomalies and trends in the western tropical Pacific, *Geophys. Res. Lett.*, *39*, L13602, doi:10.1029/2012GL052032.

Meyssignac, B., M. Becker, W. Llovel, and A. Cazenave (2012a), Assessment of two-dimensional past sea level reconstructions over 1950–2009 based on tide-gauge data and different input sea level grids, *Surv. Geophys.*, *33*(5), 945–972.

Meyssignac, B., D. S. Melia, M. Becker, W. Llovel, and A. Cazenave (2012b), Tropical Pacific spatial trend patterns in observed sea level: Internal variability and/or anthropogenic signature?, *Clim. Past*, *8*, 787–802, doi:10.5194/cp-8-787-2012.

Moon, J.-H., and T. Song (2013), Sea level and heat content changes in the western North Pacific, *J. Geophy. Res.*, *118*, 2014–2022, doi:10.1002/jgrc.20096.

Nidheesh, A. G., M. Lengaigne, J. Vialard, A. S. Unnikrishnan, and H. Dayan (2012), Decadal and long-term sea level variability in the tropical Indo-Pacific Ocean, *Clim. Dyn.*, *41*, 381–402, doi:10.1007/s00382-012-1463-4.

Penduff, T., M. Juza, L. Brodeau, G. Smith, B. Barnier, J. Molines, A. Treguier, and G. Madec (2010), Impact of global ocean model resolution on sea-level variability with emphasis on interannual time scales, *Ocean Sci.*, *6*, 269–284.

Ponte, R. (1999), A preliminary model study of the large-scale seasonal cycle in bottom pressure over the global ocean, *J. Geophys. Res.*, *104*, 1289–1300, doi:10.1029/1998JC900028.

Qiu, B. (2003), Kuroshio extension variability and forcing of the Pacific decadal oscillations: Responses and potential feedback, *J. Phys. Oceanogr.*, *33*, 2465–2482.

Qiu, B., and S. Chen (2012), Multidecadal sea level gyre circulation variability in the Northwestern tropical Pacific Ocean, *J. Phys. Oceanogr.*, *42*, 193–206, doi:10.1175/JPO-D-11-061.1.

Schneider, N., and A. J. Miller (2001), Predicting western North Pacific Ocean climate, *J. Clim.*, *14*, 3997–4002.

Shchepetkin, A., and J. C. McWilliams (2005), The regional oceanic modeling system (ROMS): A split-explicit, free-surface, topography-following coordinate oceanic model, *Ocean Modell.*, *9*, 347–404, doi:10.1016/j.ocemod.2004.08.002.

Song, Y., and D. Haidvogel (1994), A semi-implicit primitive equation ocean circulation model using a generalized topography-following coordinate system, *J. Comput. Phys.*, *115*, 228–244, doi:10.1006/jcph.1994.1189.

Song, Y. T., and T. Y. Hou (2006), Parametric vertical coordinate formulation for multiscale, Boussinesq, and non-Boussinesq ocean modeling, *Ocean Modell.*, *11*, 298–332, doi:10.1016/j.ocemod.2005.01.001.

Song, Y. T., and F. Colberg (2011), Deep ocean warming assessed from altimeters, gravity recovery and climate experiment, in situ measurements, and a non-Boussinesq ocean general circulation model, *J. Geophy. Res.*, *116*, C02020, doi:10.1029/2010JC006601.

Taguchi, B., S. P. Xie, N. Schneider, M. Nonaka, H. Sasaki, and Y. Sasai, (2007), Decadal variability of the Kuroshio extension: Observations and an eddy-resolving model hindcast, *J. Clim.*, *20*, 2357–2377.

Timmermann, A., S. McGregor, and F.-F. Jin (2010), Wind effects on past and future regional sea-level trends in the southern Indo-Pacific, *J. Clim.*, *23*, 4429–4437.

Wainwright, L., G. Meyers, S. Wijffels, and L. Pigot (2008), Examining the tropical Pacific's response to global warming, *Eos Trans. AGU*, *89*, 81, doi:10.1029/2008EO090002.

Wunsch, C., R. M. Ponte, and P. Heimbach (2007), Decadal trends in sea level patterns: 1993–2004, *J. Clim.*, *20*, 5889–5911, doi:10.1175/2007JCLI1840.1.